Using statistical models to depict the response of multi-time scales drought to forest cover change across climate zones

Yan Li[1], Henning W. Rust[1], and Bo Huang[2]

[1]Institute of Meteorology, Freie Universität Berlin, 12165, Berlin, Germany
[2]Industrial Ecology Programme, Department of Energy and Process Engineering, Norwegian University of Science and Technology, 7491, Trondheim, Norway

Correspondence: Yan Li (yan.li@met.fu-berlin.de)

Abstract.

The interaction between forest and climate exhibits regional differences due to a variety of biophysical mechanisms. Observational and modelling studies have investigated the impacts of forested and non-forested areas on a single climate variable, but the influences of forest cover change on a combination of temperature and precipitation (e.g., drought) have not been explored owing to the complex relationship between drought conditions and forests. In this study, we use the historical forest and climate datasets to explore the changes in forest fraction and drought from 1992–2018. A set of linear models and an analysis of variance approach are utilized to investigate the effect of various factors on droughts across different time scales and climate zones. Our findings reveal that precipitation is the dominant factor leading to drought in the equatorial, temperate, and snow regions, while temperature controls drought in the arid region. The impact of forest cover on droughts varies under different precipitation and temperature quantiles. Precipitation modulates forest cover's impact on long-term drought in arid and snow regions, while temperature modulates forest cover's impact on both short- and long-term drought in the arid region as well as only on long-term drought in temperate and snow regions. Forest cover can also modulate the impacts of precipitation and temperature on drought. High forest cover leads to a combined effect of precipitation and temperature on long-term drought in equatorial, arid and snow regions, while precipitation is the only dominant factor in low forest cover conditions. In contrast, low forest cover triggers a strong combined effect of precipitation and temperature on drought in the temperate region. Our findings improve the understanding of the interaction between land cover change and the climate system and further assist decision-makers to modulate land management strategies in different regions in light of climate change mitigation and adaptation.

1 Introduction

Forests cover around 4.06 billion hectares, accounting for around 30 % of the global ice-free land surface, and are distributed widely from the tropical to boreal regions (Crowther et al., 2015; Hansen et al., 2013). Global forests have undergone significant changes in the past few decades (Hansen et al., 2013). Most countries have reported a net forest loss due to intensive logging in the tropical region, especially in the 2000s. The tropical forest loss rate increased from -4040 hectares per year in the 1990s to -6535 hectares per year in the 2000s (Kim et al., 2015). At the mid-latitudes, forest cover fraction has increased owing

25 to accelerated afforestation (Hansen et al., 2013). Large deforestation areas have been detected in the boreal regions due to wildfire occurrence (Hansen et al., 2010). At the national scale, China contributes to the largest afforestation area in the world, as more than 16 sustainability programs have been launched in the country since the 1970s (Bryan et al., 2018). The area of planted forest in China has increased by around 1.7 million hectares per year since the 1990s (Peng et al., 2014). Brazil has been the world leader in tropical deforestation, clearing an average of approximately 1.95 million hectares per year from 1996

30 to 2005 (Nepstad et al., 2009). The global forest areas are predicted to change from about –500 million hectares up to +1000 million hectares by the end of the 21st century under five different Shared Socio-economic Pathways (SSPs) (Popp et al., 2017).

Forests play a vital role in supporting ecosystem services, including local climate regulation via water and heat exchanges with the atmosphere (known as biophysical effects) (Anderson et al., 2011; Bonan, 2008). Changes in forest cover have the potential to alter local climate by affecting surface evapotranspiration, albedo and surface roughness (Alkama and Cescatti,

35 2016; Mahmood et al., 2014). The net impact on local climate is highly spatially heterogeneous due to the balance among these mechanisms (Perugini et al., 2017; Li et al., 2015; Cherubini et al., 2018). In general, afforestation in the tropics results in regional land surface cooling due to high evapotranspiration, while the effect is warming in the boreal region caused by forests typically having a low surface albedo, especially in the snow-covered winter (Alkama and Cescatti, 2016; Perugini et al., 2017). At mid-latitudes, the effects are more uncertain and have more spatial variability, particularly at a local scale (Mahmood et al.,

40 2014; Perugini et al., 2017; Findell et al., 2017). The uncertainties are mainly caused by the regional background conditions (climate and soil moisture), forest types (coniferous vs. deciduous), types of land used for comparison (cropland vs. grassland), or analysis methods (observations vs. climate models) (Ge et al., 2019; Li et al., 2016; Pitman et al., 2011; Tian et al., 2022). For instance, a study using satellite retrieval products shows that the non-radiative (i.e., evapotranspiration) effect dominates in surface cooling in a typical temperate region (i.e. the Loess Plateau in China) (Ge et al., 2019). Nevertheless, for the same

45 region, a coupled land-atmosphere model finds a net surface warming caused by radiative effects (i.e., changes in surface albedo and radiation fluxes) (Tian et al., 2022).

Forest change also can influence the hydrologic cycle by altering evapotranspiration, streamflow, precipitation, and soil moisture (Bonan, 2008; Hoek van Dijke et al., 2022). Deforestation in the tropics can result in a strong decrease in precipitation, with up to 30 % of annual total precipitation (Snyder et al., 2004; Perugini et al., 2017). This is because more than half of

50 forest evapotranspiration can be recycled and produce rainfall in this region (Salati and Nobre, 1991; Silva Dias et al., 2009). In the boreal region, tree removal leads to a slight reduction in precipitation, around 15 % of the annual total precipitation (Snyder et al., 2004; Cherubini et al., 2018). This is likely due to inappreciable differences in the evapotranspiration ratio between different vegetation covers in boreal region (Beringer et al., 2005). Forests' change impacts on precipitation in the temperate regions are more complex than in the boreal or tropical region (Bala et al., 2007; Field et al., 2007; Bonan, 2008).

55 It is challenging to detect the signal of forest cover changes on rainfall in the temperate region, owing to the high variability of synoptic scale meteorological systems, which impact local-to-regional circulation and rainfall patterns (Bala et al., 2007; Field et al., 2007; Bonan, 2008). Modelling studies suggest that a decline in vegetation cover can lead to a reduction in annual precipitation in this region, ranging from -73 to -219 mm per year (Perugini et al., 2017).

Changes in temperature and precipitation may affect regional wet and dry conditions, such as drought. Drought is a complex
60 climatic phenomenon characterized by below-normal rainfall over a period from months to years (Dai, 2011). And it is mainly
driven by a combined effect of temperature, precipitation, wind speed, and solar radiation (Seneviratne, 2012). Meanwhile,
drought is also considered a natural disaster that poses serious threats to ecosystems by changing the forest structure and
carbon content (Nepstad et al., 2007). Moreover, several studies have reported changes in drought characteristics in the past
few decades (Cook et al., 2014; Trenberth et al., 2014; Naumann et al., 2018; Zhao and Dai, 2015). For example, since the
65 1950s, the frequency and intensity of droughts have increased in the Mediterranean (Vicente-Serrano et al., 2014) and West
Africa (Dai, 2013), while there has been a small increase in central North America (Peterson et al., 2013) and northwest
Australia (Jones et al., 2009).

Some studies have indicated that alterations in forest cover are highly likely to have an impact on regional drought conditions.
For example, deforestation leads to less water that can be recycled and intensifies the regional dry seasons in the Amazon region
70 (Bagley et al., 2014; Staal et al., 2020). Based on model simulations, the conversion of mid-latitude natural forests to cropland
and pastures is accompanied by an increase in the occurrence frequency of hot-dry summers (Findell et al., 2017). To date, no
reports have addressed the impact of forest changes on drought conditions in other regions. Additionally, the different time-
scale drought responses to forest change have not been explored. Given the significance of forest management decisions for
climate adaptation and mitigation targets, it is essential to comprehend how drought responds to alterations in forest cover. In
75 this study, we aim to employ statistical models to explore the connection between forest cover changes and drought, keeping
the following questions in mind:

1. How do changes in forest cover affect droughts at different time scales?

2. What is the role of forest cover change in modulating drought across various climatic regions?

The objective of this study is to give a fundamental view of the relationship between observational forest change and drought
80 change to understand how drought responds to forest change across different time scales and climate zones. A brief introduction
involving forest change and its climate effect is given in Section 1. Section 2 presents an overview of the data description and
source, followed by a discussion on methods used in the paper in Section 3. Section 4 evaluates the effect of forest cover change
on drought in different time scales and climate zones. Section 5 concludes the main findings along with the limitation and the
possible extension of the work.

2 Data

2.1 Climate Classification

The climate classification is based on the latest digital Köppen-Geiger World map dataset (Peel et al., 2007) (http://www.
hydrol-earth-syst-sci.net/11/1633/2007/hess-11-1633-2007-supplement.zip), which was first formulated by Wladimir Köp-
pen and has been updated for several generations. The philosophy behind the construction of this new version is to rely on

90 observed data rather than experience, wherever this is possible, to minimize the number of subjective decisions. The map

dataset is defined on long-term station records of monthly precipitation sums and monthly mean temperature obtained from the

Global Historical Climatology Network (GHCN) version 2.0 dataset (Peterson and Vose, 1997). In the creation of the climate

classification dataset, 12,396 precipitation stations and 4,844 temperature stations were used, and there are 30 possible climate

types. We aggregate the 30 climate types into five main climate groups, defined as *equatorial*, *arid*, *temperate*, *snow* and *polar*

95 region. These regions are depicted in detail in Fig. 1. In this paper, only the first four regions are considered, as forest cover in

the polar region is negligible.
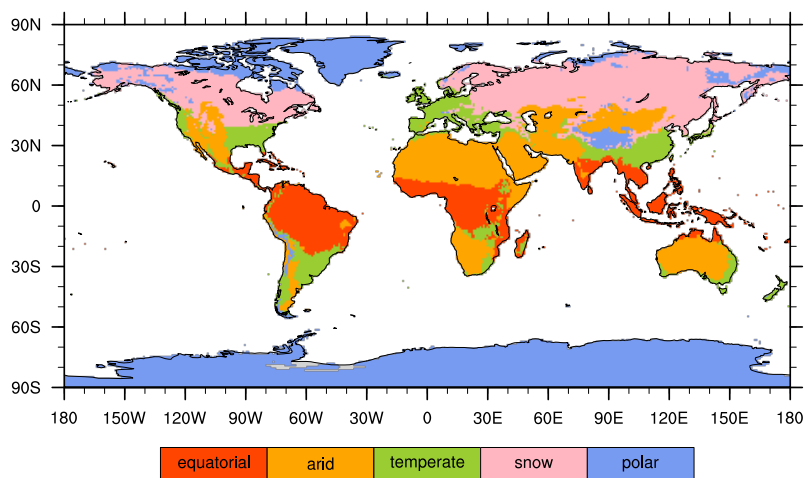
Figure 1. Global distribution of main climate classification, according to Köppen- Geiger World map.

2.2 Drought Indices

To measure, monitor and analyse the drought, multi indices have been developed (Keyantash and Dracup, 2002). Over the

past few decades, there are two widely-used drought indices, the *Standardized Precipitation Evapotranspiration Index* (SPEI)

100 (Vicente-Serrano et al., 2010a) and the *self-calibrating Palmer Drought Severity Index* (scPDSI) (Burke et al., 2006). These two indices describe the effect of temperature and precipitation on droughts. Furthermore, the SPEI describes droughts at different time scales, which is important for our first research question. The SPEI focuses more on atmospheric conditions, while scPDSI takes the situation in the soil into account. In order to obtain a more comprehensive picture, both indices are therefore used in this study.

2.2.1 The Standardized Precipitation Evapotranspiration Index (SPEI)

The SPEI is the extension of the SPI (*Standardized Precipitation Index*), which maps the precipitation intensity on a Gaussian variable and uses precipitation (P) as the only input (McKee et al., 1993). Moreover, the SPEI additionally considers the influence of potential evapotranspiration (PET) and uses the difference between P and PET, and it is a time-scale dependent drought index. For this, we specify an integration time scale τ and a reference month, e.g. SPEI03 for May denotes a drought

110 index obtained for the period from March to May.

The global SPEI dataset used in this study is available as monthly values with a spatial resolution of $0.5° \times 0.5°$. We choose to download various integration time scales τ of the index: 3 months (SPEI03, short-term), 6 months (SPEI06, mid-term), 12 months (SPEI12, mid-term) and 24 months (SPEI24, long-term). The time period considered is 1992-2018. The calculation of PET is based on the FAO-56 Penman-Monteith method (Allen et al., 1998).

115 Data was downloaded from *SPEIbase v.2.6* in March 2020 (Vicente-Serrano et al., 2010b, a) (http://digital.csic.es/handle/10261/202305). The dataset is based on the Climatic Research Unit (CRU) TS 4.03 precipitation and potential evapotranspiration data.

Each grid point is then associated with one of the 5 regions given in Fig. 1. Averaging over all grid points in one region yields the SPEIτ at monthly resolution for a given region; subsequently averaging over all months of a year yields annual values for

120 each region, e.g., the SPEI03 for the year 2000 is the average over the SPEI03 from January to December of the same year.

2.2.2 The self-calibrating Palmer Drought Severity Index (scPDSI)

The Palmer Drought Severity Index (PDSI) is an old drought indicator, developed in 1965 to assess the soil's moisture available by using precipitation and temperature to estimate moisture supply and demand within a two-layer soil model (Wayne, 1965). In 2004, Wells et al. (2004) developed the PDSI into scPDSI, more effectively improving the comparability of the index at

125 different locations. As with the PDSI, the scPDSI is calculated from time series of precipitation and temperature, together with fixed parameters related to the soil/surface characteristics at each location. The fundamental calculation of PET follows Thornthwaite's method (Thornthwaite, 1948). In 2006, Burke et al. (2006) improved the calculation of PDSI, using the Penman-Monteith approach (Maidment et al., 1993) to establish the evapotranspiration, which is applied to the actual vegetation cover, rather than a reference crop (as is done implicitly in the Thornthwaite's method).

130 The scPDSI dataset is available at a $0.5°$ resolution at monthly resolution for the time period 1992-2018. It is based on the CRU TS 4.05 dataset and the calculation of PET is based on the Penman-Monteith method. The dataset was downloaded from https://crudata.uea.ac.uk/cru/data/drought/ in March 2021 (Barichivich et al., 2021; van der Schrier et al., 2013). Each

grid point is associated with one of the 5 regions given in Fig. 1. Averaging the scPDSI over all grid points in a region and subsequently averaging all months of the year yields the annual scPDSI for the region.

2.3 Forest Cover

Changes in forest cover fraction are calculated based on the annual European Space Agency (ESA) Climate Change Initiative (CCI) land cover maps from 1992 to 2018 at a spatial resolution of 300 m. Land cover dataset was downloaded from http://maps. elie.ucl.ac.be/CCI/viewer/download.php (Santoro et al., 2017) as *Land Cover CCI Climate Research Data Package* (CRDP) in June 2021. The maps describe the earth's terrestrial surface in 37 land cover classes based on the United Nations Land Cover Classification System (UNLCCS), and 14 out of the 37 classes are defined as forest. The dataset was produced after the combination of the global daily surface reflectance of five different satellite observation systems, with the ambition to maintain high levels of consistency over time. It has high accuracy (>70 %) in representing cropland classes, forests, urban areas, bare areas, water bodies and perennial snow and ice (Poulter et al., 2015). This dataset has been widely used in investigating recent land cover change and its climate effect (Huang et al., 2020; Hu et al., 2020). We aggregated the dataset to a $0.5° \times 0.5°$ resolution, and at each grid point, the forest fraction can take values between 0 and 1. In the following, we use forest fraction aggregated to the level of regions, centered and scaled the annual values by their standard deviation to unit variance for the sake of visualizing the interannual change and comparing the contribution of forest fraction change in linear models (Sect. 4) to other analogously scaled variables.

Fig. 2 shows the time series of annual forest fraction (centered and scaled to unit variance) for the four regions (equatorial, arid, temperate and snow) as well as the drought indices (scPDSI, SPEI03, SPEI06, SPEI12 and SPEI24) for the period from 1992 to 2018.

In the equatorial region, the forest fraction declines monotonously until 2013 with the decay being slower since 2004. Since then, it is slightly increasing. From the visual comparison, there is no obvious relation to any of the drought indices. In the arid region, forest fraction declines until 2003 and increases again, interrupted by a few years of decline around 2010. The regeneration to (and even above) values from 1992 happens relatively quickly since 2016. Drought indices are all negative since about 1998 and fluctuate around a relatively constant value since 2010. The temperate zone also show a decline in forest fraction until 2003, followed by slight ups and downs until 2015. In the last years until 2018, the forest fraction has increased again to the average level. Compared to the plots in other regions, the drought indices in the snow zone undulate around zero (coordinate on the right y-axis), and there is little difference between SPEI and scPDSI. The forest fraction bars show an almost opposite behavior as in other regions: an increase until around 2009 followed by a decrease leveling off at around 2016.

2.4 Precipitation and Temperature

Climatic Research Unit (CRU) monthly near-surface temperature and precipitation datasets are downloaded in March 2021 and used in this study. They are gridded datasets with a spatial resolution of $0.5° \times 0.5°$. In the CRU datasets, meteorological station observations were interpolated to grids and given as monthly values by an automated method. It is publicly available
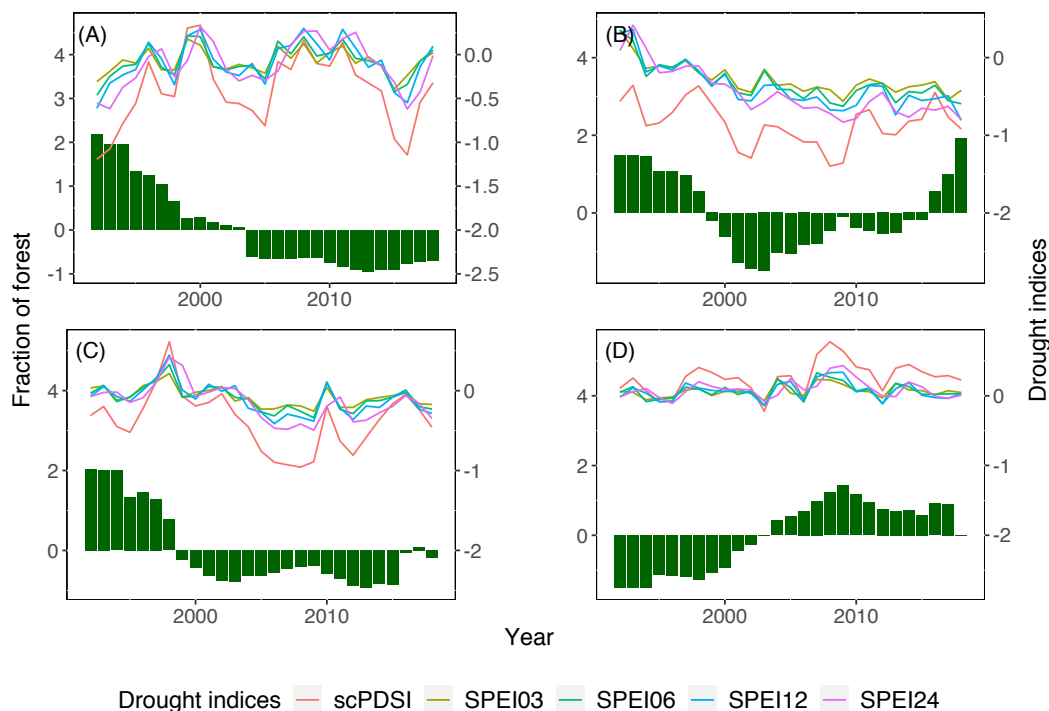
Figure 2. Annual change in forest fraction (centered and scaled to unit variance, green bars) and drought indices (colored lines, see legend) from 1992 to 2018 across 4 regions: (A) equatorial; (B) arid; (C) temperate; (D)snow.

165 (https://crudata.uea.ac.uk/cru/data/hrg/) and is referred as CRU TS v. 4.03 (Harris et al., 2014). The datasets are used to analyse the effect of meteorological factors on droughts.

Again, for the sake of easier comparison, the variables in Fig. 3 have been centered and scaled to unit variance. Shown is the annual mean of monthly precipitation as bars and temperature as black dots for the different climate zones (different columns) in Fig. 3 together with the drought indices considered here (different rows). Note that for the SPEI for 3, 6, 12 and
170 24 months, temperature and precipitation are analogously aggregated to this length. Hence, for SPEI06 in June, we average monthly precipitation and temperature from January to June and for SPEI06 for July, from February to July and so on. Fig. 3 shows the annual means of precipitation and temperature aggregated analogously to the aggregation level of the drought index.

In equatorial and temperate regions, the main influencing factor to droughts is precipitation, which is largely consistent with changes in the drought index; while this relationship is not visible for the arid region, where the temperature has a larger
175 influence. In snow regions, the situation is even more complex. Furthermore, Fig. 3 also gives an idea about the difference between scPDSI and SPEIs. In equatorial, temperate and snow regions, the change of scPDSI and SPEI is similar; but in the arid region, the variation is different. This is probably due to the low precipitation in the arid region, causing a large difference in the water content of the atmosphere and soil.
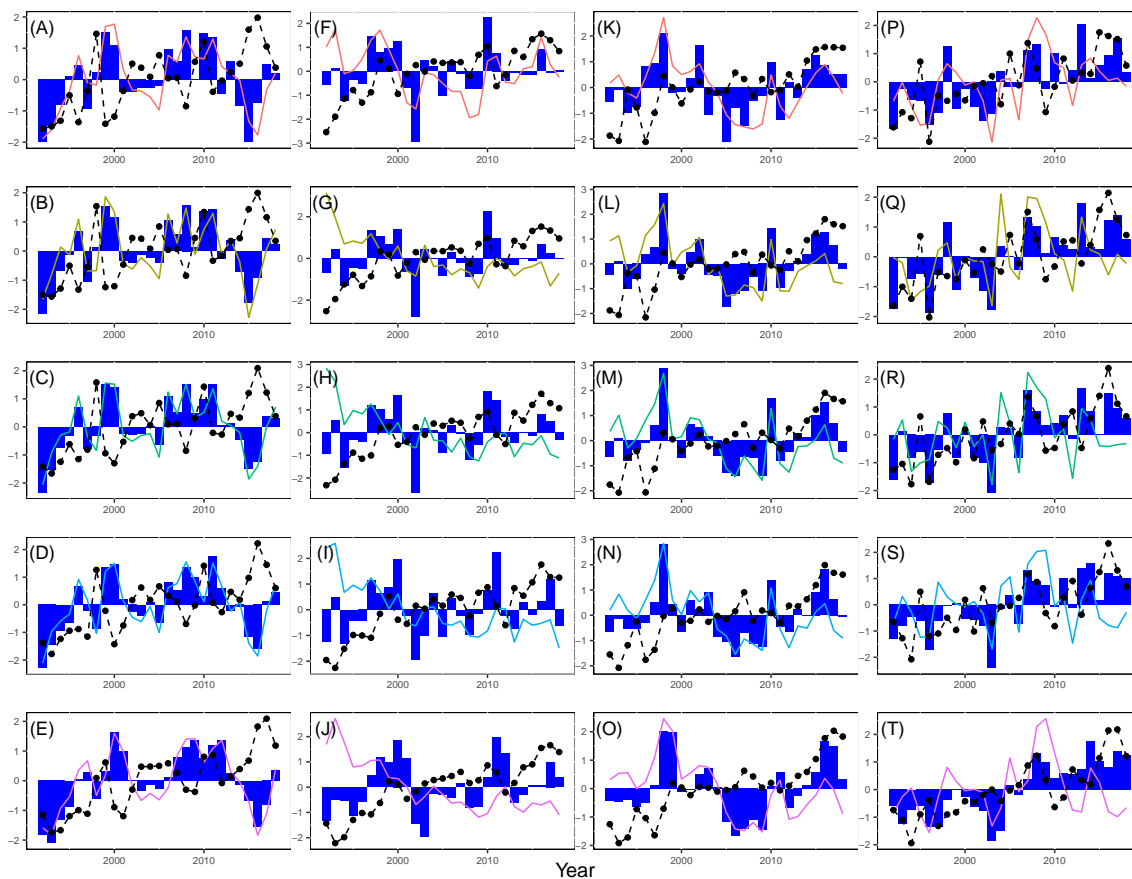
Figure 3. Time series of regional averaged annual precipitation (bar), temperature (dashed line) and Drought indices (lines, the legend is the same with Fig. 2; rows from top to bottom: scPDSI and SPEIτ with $\tau \in \{03, 06, 12, 24\}$) from 1992 to 2018 across different zones (columns from left to right: equatorial, arid, temperate, snow)

3 Methods

3.1 Linear Models

We use linear models to explore the influence of forest cover, as well as temperature and precipitation on the drought indices in various climate zones. Linear models allow the assessment of drought indices for hypothetical situations in a projected climate change scenario. The target variable (drought index) is assumed to be a realization of a normally distributed random variable Y with constant variance σ^2 and varying expectation μ

$$Y \sim \mathcal{N}(\mu, \sigma^2). \tag{1}$$

The expectation μ depends on a set of covariates (or independent variables) $X_1, X_2, X_3, \ldots, X_p$, which we expect to influence the expectation of the target (drought index) in a linear way,

$$\mu = \beta_0 + \beta_1 X_1 + \beta_2 X_2 + \beta_3 X_3 + \ldots \beta_p X_p. \tag{2}$$

The unknown model parameters β_i are estimated using maximum-likelihood (Wilks, 2019), realized within the environment for statistical computing R (R Core Team, 2018) using the function lm() (Chambers and Hastie, 1992; Wilkinson and Rogers, 1973) from the package stats.

For ease of communication, we adopt the notation for linear models introduced by McCullagh and Nelder (1989). For example, for a model with covariates X_1, X_2, X_3 which enter all as direct effects and $X_2 X_3$ as interactions, i.e.

$$\mu = \beta_0 + \beta_1 X_1 + \beta_2 X_2 + \beta_3 X_3 + \beta_4 X_2 X_3, \tag{3}$$

the model notation reads

$$Y \sim X_1 + X_2 * X_3 = X_1 + X_2 + X_3 + X_2 : X_3, \tag{4}$$

with $X_2 * X_3$ being shorthand for $X_2 + X_3 + X_2 : X_3$, i.e. including X_2 and X_3 as direct effects and as interaction $X_2 : X_3$.

Here, we use

$$D_\tau \sim X_{\text{forest}} + X_{\text{precip}} + X_{\text{temp}} + X_{\text{forest}} : X_{\text{temp}} + X_{\text{forest}} : X_{\text{temp}} + X_{\text{precip}} : X_{\text{temp}}, \tag{5}$$

with D_τ denoting the drought index, i.e. scPDSI or SPEI with integration time τ, X_{forest} the forest cover fraction, X_{precip} the annual mean precipitation and X_{temp} the annual temperature mean. $X_a : X_b$ denote interactions, e.g. $X_{\text{forest}} : X_{\text{temp}}$ describes the influence of temperature depending on forest cover fraction. All variables are standardized to zero mean and unit variance prior to parameter estimation.

The SPEI is a time-scale dependent drought index with integration time τ. Note that the integration time τ also defines the first available data point for D_τ as $\tau - 1$ month after the start of the time series in January 1992. Thus for longer integration times, the SPEIτ cannot be obtained for the first years of the data set, e.g. for SPEI24, the calculation starts in December of the second year.

Based on Eq. 5, we estimate the impact of forest fraction and meteorological factors on drought. For SPEI03, SPEI06 and SPEI12 of a specific month, we use the previous 3, 6 or 12 months' data; for SPEI24, we do need the data of the previous 2 years.

Fig. 4 compares annual values for the SPEIτ obtained as described in Sec. 2.2 (points) to the expectation from the linear models (Eq. 5 using forest fraction X_{forest}, temperature X_{temp} and precipitation X_{precip} as inputs (lines); the rows give the scPDSI and the SPEIτ for different integration time scales $\tau \in \{03, 06, 12, 24\}$ (from top to bottom) and across various climate zones (columns, equatorial, arid, temperate, snow, from left to right). And in Tab. 1, we also give MSE (Mean Squared Error) and Adjusted R^2 for all models in Fig. 4.

The Mean Squared Error (MSE) quantifies the difference between model estimates and observed values for the drought indices, computed as,

$$MSE = \frac{1}{n}\sum_{i=1}^{n}(y_i - \widehat{Y}_i)^2 = \frac{1}{n}\sum_{i=1}^{n}(D_{\tau,i} - \widehat{D_{\tau,i}})^2 \,, \tag{6}$$

with y_i representing the observed values for the drought index ($D_{\tau,i}$, scPDSI and SPEIs), $\widehat{Y}_i$ denote the model estimates ($\widehat{D_{\tau,i}}$),

220 n the number of data points, i.e. the number of years. The coefficient of determination R^2 gives the fraction of variability described by the model

$$R^2 = \frac{SS_{\text{reg}}}{SS_{\text{tot}}} = 1 - \frac{SS_{\text{res}}}{SS_{\text{tot}}} \tag{7}$$

with the total sum of squares

$$SS_{\text{tot}} = \sum_{i=1}^{n}(y_i - \overline{y_i})^2 = SS_{\text{reg}} + SS_{\text{res}} \,, \tag{8}$$

225 the sum-of-squares of the regression

$$SS_{\text{reg}} = \sum_{i=1}^{n}(\widehat{Y}_i - \overline{y_i})^2 \,, \tag{9}$$

the sum-of-squares of the residuals

$$SS_{\text{res}} = \sum_{i=1}^{n}(y_i - \widehat{y_i})^2 \,, \tag{10}$$

and $\overline{y_i}$ denoting the arithmetic mean of the observations y_i. We use the adjusted R^2

230 $$R^2_{\text{adj}} = 1 - \frac{SS_{\text{res}}/df_{\text{res}}}{SS_{\text{tot}}/df_{\text{tot}}} = 1 - \frac{\sum_{i=1}^{n}(y_i - \widehat{Y}_i)^2/(n-1-p)}{\sum_{i=1}^{n}(y_i - \overline{y_i})^2/(n-1)} \,, \tag{11}$$

with df_{tot} and df_{res} denoting the degrees of freedom for the total and residual sum-of-squares, respectively, n the number of observations and p the number of covariates (independent variables).

The linear model is able to capture the inter-annual variability of the drought indices to a certain extent with performance varying across climate zones. From visual inspection and comparison of R^2_{adj}, drought indices in the equatorial region can be

235 described best ($0.84 < R^2_{\text{adj}} < 0.97$), while for the snow region ($0.23 < R^2_{\text{adj}} < 0.39$), the model is by far not as performant, cf. Tab. 1. For arid and temperate zones, the models are almost as performant as for the equatorial zone. The MSE in the equatorial region is around 0.1 and smaller, while in the snow region, we find MSE of around 0.5 (Tab. 1). Thus in the equatorial, temperate and arid regions, linear models with two-point interactions of forest cover, temperature and precipitation are well suited to describe the drought indices used here; whereas in the snow region, the factors influencing the drought indices

240 must be more complex than this.

Furthermore, we see from Fig. 4 and Tab. 1 that the SPEI indices with varying time scale τ are consistently better represented by the model (larger R^2_{adj}) than the scPDSI over all regions, with performance (R^2_{adj}) roughly increasing with τ (except for the snow region). We hypothesize that this is an effect of the calculation of the scPDSI based on a 2-layer soil box model and thus local soil conditions are relevant; the latter are not represented in our model-building process.
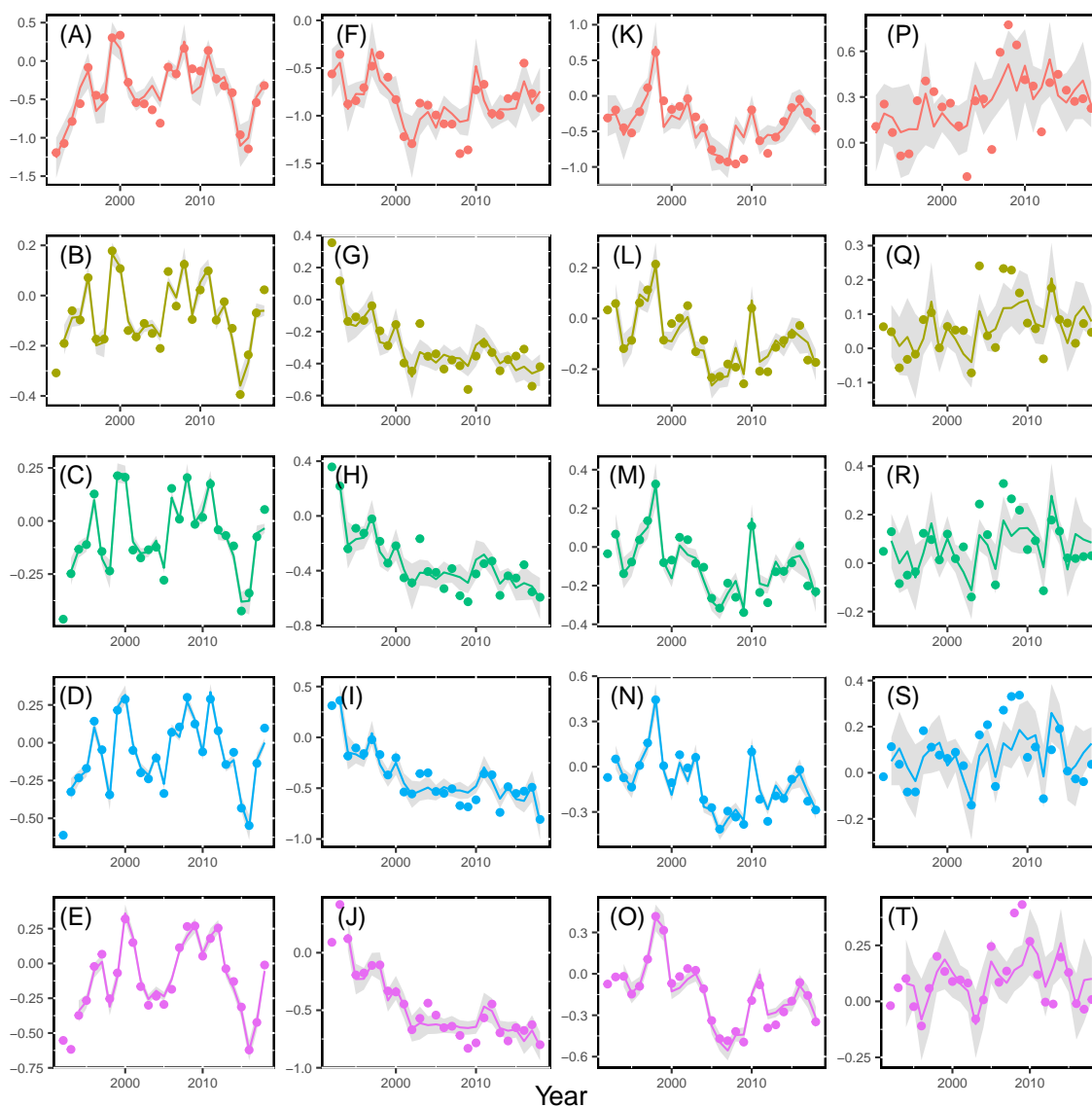
Figure 4. Time series of drought indices (colors as same as in Fig. 2); annual point estimates (points) and estimates from the linear model (Eq. 5, lines) across different climate zones (columns from left to right: equatorial, arid, temperate, snow) and for the scPDSI and SPEIτ with different integration times (rows from top to bottom: scPDSI and SPEIτ with $\tau \in \{03, 06, 12, 24\}$). The shade signifies the range lies at a 95% level of confidence. Note that SPEI03, SPEI06 and SPEI12 cannot be obtained for the first year and SPEI24 can not be obtained for the first 2 years.

Table 1. MSE (Mean Squared Error) and Adjusted R^2 (R^2_{adj}) for all models in Fig. 4.

	Equatorial region		Arid region		Temperate region		Snow region	
	MSE	R^2_{adj}	MSE	R^2_{adj}	MSE	R^2_{adj}	MSE	R^2_{adj}
scPDSI	0.12	0.84	0.31	0.59	0.23	0.70	0.57	0.23
SPEI03	0.05	0.93	0.17	0.77	0.10	0.86	0.49	0.32
SPEI06	0.03	0.95	0.17	0.76	0.09	0.88	0.45	0.39
SPEI12	0.03	0.97	0.11	0.85	0.05	0.94	0.53	0.27
SPEI24	0.02	0.97	0.09	0.87	0.04	0.94	0.53	0.27

3.2 Analysis of Variance

Analysis of variance (ANOVA Anscombe, 1948) gives a quantitative estimate of the relative strength of these factors, which is used to quantify the effect of the various covariates X. We use it to describe the drought indices with, i.e. forest fraction, precipitation and temperature, cf. Eq. 5. We denote the full model for a drought index D as D_{full} as given in Eq. 5. The model without the information on the forest is denoted as

$$D_{\text{-forest}} \sim X_{\text{precip}} * X_{\text{temp}} \,, \tag{12}$$

analogously, we denote models without information on temperature or precipitation as $D_{\text{-temp}}$ and $D_{\text{-precip}}$, respectively. With

$$SS_{\text{forest}} = SS_{reg}(D_{\text{full}}) - SS_{reg}(D_{\text{-forest}}), \tag{13}$$

we assess the improvement in model performance in terms of regression sum-of-squares due to including the forest fraction as a covariate, with the F-test giving significance to that. Note that the difference in degrees of freedom used in the F-test for the full and the reduced model is $\delta p = 3$ as all terms in Eq. 5 involving forest fraction X_{forest} are taken out. Analogously, we define SS_{temp} and SS_{precip} for quantifying the influence of temperature and precipitation.

The fraction of variance contributed to the regression by forest fraction is given as

$$\Delta SS_{\text{forest}} = \frac{SS_{\text{forest}}}{SS_{reg}(D_{\text{full}})} \,, \tag{14}$$

analogously for precipitation ($\Delta SS_{\text{precip}}$) and temperature ($\Delta SS_{\text{temp}}$).

4 Results

The gridded monthly data have been averaged to annual regional mean values according to the climate classification in Fig. 1. In the following, we analyze four regions: equatorial, arid, temperate and snow. For each region, linear models for scPDSI, SPEI03, SPEI06, SPEI12 and SPEI24 are built to describe the relationship between the drought indices (D_τ) and 3 covariates

(factors) (X_{forest}, X_{precip}, X_{temp}). The annual values for forest fraction X_{forest} and the SPEIτ have a time delay, as discussed
in Sec. 3: the model for SPEI03, SPEI06 and SPEI12 uses meteorological data from 1993 to 2018 while the values for forest
fraction are from 1992 to 2017; the model for SPEI24 uses meteorological data from 1994 to 2018, while values for forest
fraction are from 1992 to 2016; for scPDSI, all values for the covariates are from 1992 to 2018. Here, the results in terms of
the proportion of variance added to the models by forest cover change and other meteorological factors across different regions
are displayed first. Subsequently, we investigate the interaction of the three factors on droughts in four regions. Key insights
emerging from the results are discussed and we also give some possible explanations.

4.1 The proportion of variance described by forest cover change

Based on the linear models for all variants of drought indices and across climate zones, we estimate the contribution of the 3
covariates to the regression according to the procedure described in Sec. 3.2. The bars in Fig. 5 show the proportion of variance
contributed by forest cover fraction (X_{forest}, green), precipitation (X_{precip}, blue), and temperature (X_{temp}, red) to the regression.
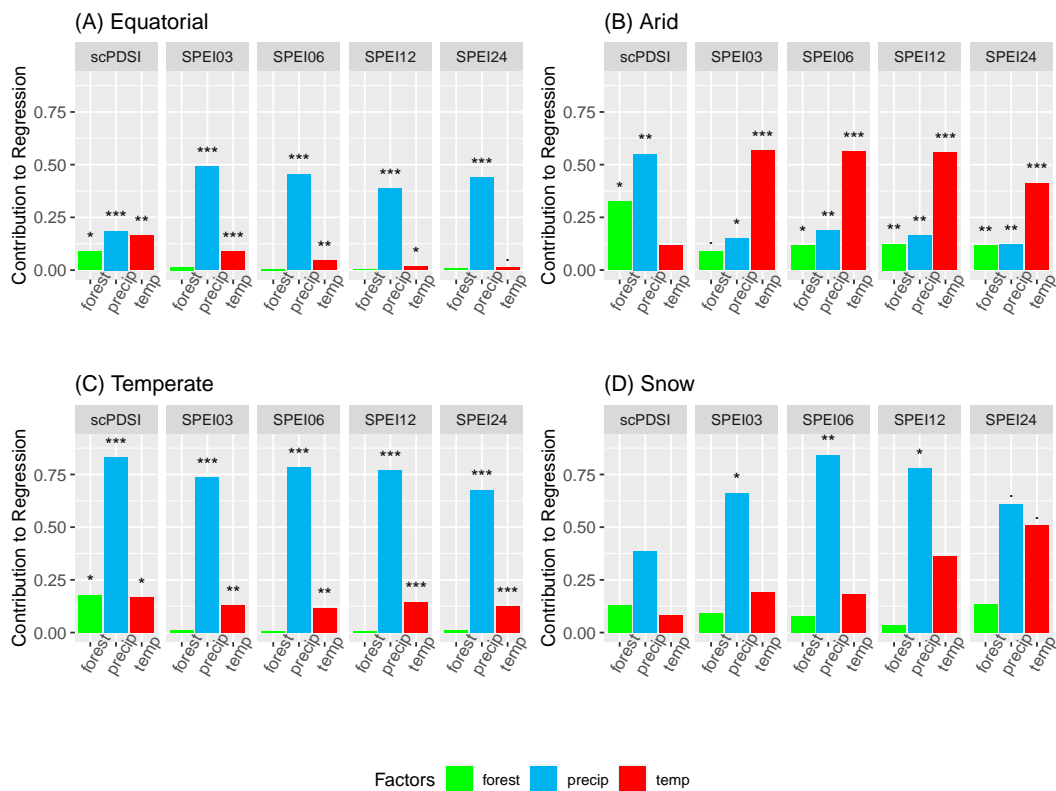
Figure 5. Proportion of variance contributed by forest fraction, precipitation, and temperature to the full model that describes drought indices
at different time scales across 4 climate regions. (confidence significant level at '***' 0.001, '**' 0.01, '*' 0.05, '.' 0.1.)

275   The contribution of precipitation to variability ominates for drought indices in equatorial, temperate, and snow regions.
For the arid region, precipitation only dominates scPDSI, while for SPEI-based drought indices, temperature dominates its
variability here. For the temperate region, precipitation contributes the largest fraction of variance compared to other regions,
followed by the snow region.

For the equatorial and temperate regions, the forest fraction describes a more significant fraction of the regression variance for scPDSI than for
280   the SPEI-based drought indices. As scPDSI is the only drought index used here which involves soil properties, we hypothesize
that forest fraction is linked to these and thus has some potential to describe more about the variability of scPDSI. However,
we still should note that the linear models better represent SPEI-based indices (higher R^2_{adj} in Tab. 1) than scPDSI.

For the equatorial and temperate regions, forest fraction does not contribute to describing the variability of the SPEI-based
indices (non-significant). In the arid region, however, the proportion of variance contributed by forest cover to SPEI-based
285   indices is around 0.1 and at least significant on the 0.05 level (SPEI03 only on 0.1 level). While for the snow region, the con-
tributing fraction of variance is comparably large but not statistically significant on any reasonable level. Here, the contribution
of precipitation is particularly large for SPEI06 and the influence of temperature seems to increase with time scale τ, however,
the latter is not significant on the normal levels. Thus for the snow region, precipitation seems to have a larger impact on
short-term drought indices while temperature affects more long-term indices. Note that the linear models for the snow region
290   show adjusted R^2 values of around 0.3 and hence are a lot less capable of describing the index variability than that in other
regions ($R^2_{\mathrm{adj}} \geq 0.7$), cf. Tab. 1. Processes in the snow region seem to be more complex than what can be represented with the
approach here.

Proportions of contribution do vary across regions and drought indices: precipitation has a large influence in all regions
except the arid region; the temperature has a larger influence on SPEI-based drought indices in the arid region; forest fraction
295   describes a larger fraction of the regression variance for scPDSI than for the SPEI-based indices. Thus in the arid region, where
the ecosystems are fragile and highly vulnerable to climate change, the forest fraction has a stronger impact on changes in
drought indices.

4.2   Variations in droughts response to forest fraction according to different precipitation and temperature quantiles

Fig. 6 explores the effect of forest cover fraction on SPEI24 and SPEI03 conditioned on precipitation and temperature. Again,
300   this analysis is based on the previously discussed models. The first two rows show the effect of forest cover on SPEIs for differ-
ent levels of precipitation (dark green lines) with temperature held fixed at its median. For the bottom two rows, precipitation
has been held fixed at its median and the forest cover effect for various levels of temperature (dark yellow lines) is explored.
The strength of the colored bands is associated with the quantiles of precipitation/temperature. The dark green/dark yellow part
of the band covers the central part of the precipitation /temperature (0.4 to 0.6-quantile). For each successive outer band the
305   quantile level for temperature/precipitation changes by 0.05.

The first row of Fig. 6 (SPEI03) shows only a minor influence of forest fraction for various levels of precipitation (lines
are close to horizontal) indicating that precipitation does not modulate the influence of forest cover on the short-term drought
index. This is different for the second row (SPEI24), where a strong influence of precipitation on the forest fraction effect for
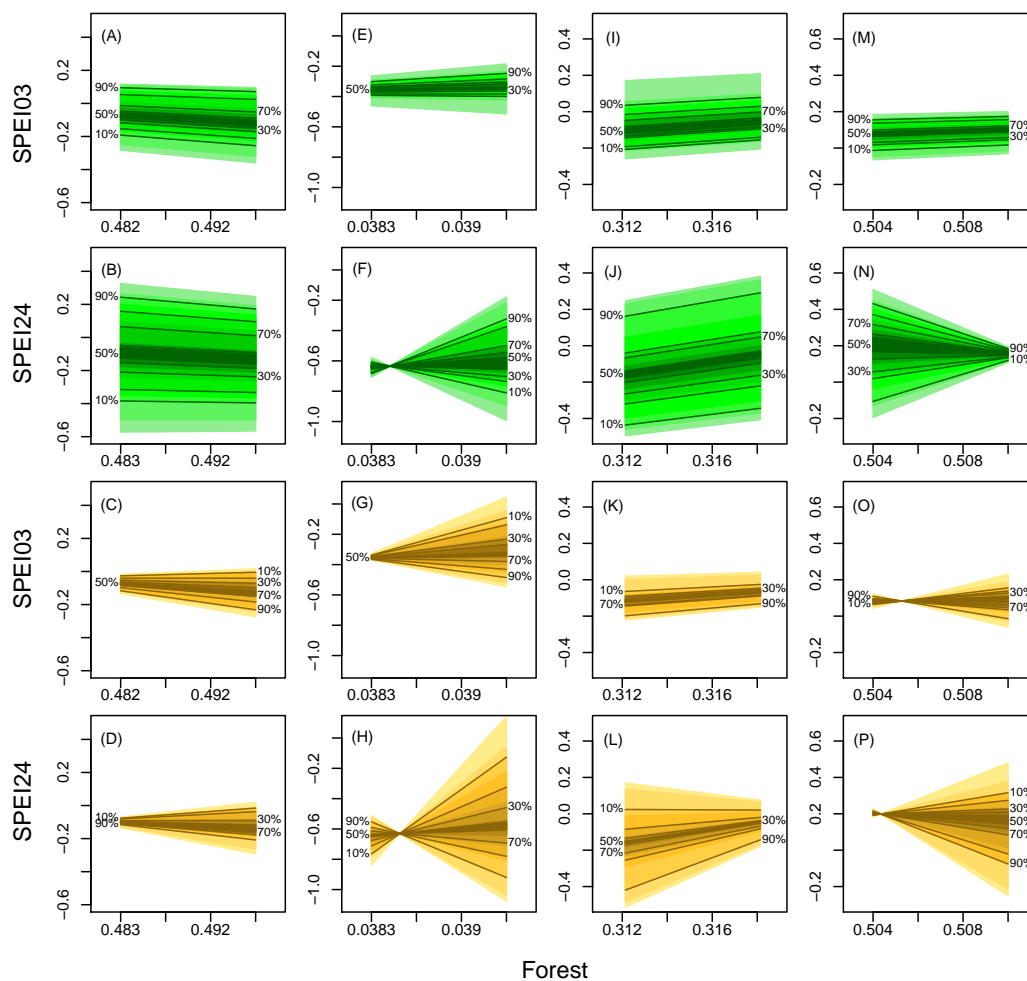
Figure 6. The effect of forest fraction on droughts for SPEI03 in the first and third rows; for SPEI24 in the second and fourth rows for different levels of precipitation (blue lines) and temperature (red lines) using the model from Sec. 3 across different climate zones (from left to right: equatorial, arid, temperate, snow). For the first two rows, the temperature is held constant at its 0.5 quantiles and the forest cover effect is explored under different quantiles of precipitation. For the bottom two rows, precipitation is held constant and the effect is shown under different temperature quantiles.

the arid region (Fig. 6F) is noted: for precipitation more than about median, the drought index increases with forest cover and

310   decreases if precipitation is less than the median. If precipitation is low and forest cover high, a low SPEI24 may be the result of a small amount of water being transpired into the atmosphere due to a high fraction of available trees. For high precipitation amounts instead, a larger forest cover would hold the water vapor, and make the SPEI24 high. The opposite effect can be observed for the snow region (Fig. 6N): for little forest cover, precipitation directly affects the SPEI24 leading to a more humid situation with more precipitation. For a higher forest cover, this effect vanishes. Recall, that for the snow region, the model

315   captures less than 30% of the total variability.

    The modulation of forest cover by temperature (Fig. 6, two bottom rows) is more diverse. In the equatorial region (Fig. 6C and D), the temperature influence is a lot weaker than precipitation (cf. Fig. 5), hence precipitation dominates the drought index in the equatorial region. However, for the higher temperature, we see a slight decrease in SPEI24 (Fig. 6D) with forest cover, while for the low temperature, SPEI24 increases with forest cover. This modulating effect of the forest cover effect on

320   the drought index is a lot stronger for the arid region. For the short-term index (SPEI03, Fig. 6G), high/low temperatures lead to a notable decrease/increase in forest cover, while the same effect is even stronger for the long-term index (SPEI24, Fig. 6H). A possible explanation is that rising temperature leads to increasing transpiration from trees, and if there are more trees, more water will be taken away, and the drought indices will decrease. For low temperatures, the forest transpiration will be weak and if there are more trees, exposed surface area decreases, and less water will be taken away (Shaxson and Barber, 2003).

325   A simulation about soil evaporation has been carried out in Kenya (in an arid region), which found that trees could reduce annual soil evaporation directly beneath their canopy by an average of 35% (compared to completely bare soil), equivalent to 21% of rainfall over there (Wallace et al., 1999). For the temperate zone, high temperatures lead to an increase in drought index with forest cover, possibly because precipitation is always sufficient in this location and the types of trees here can adapt their leaves and roots to absorb all of the excess water, with the effect being stronger for SPEI24 (Fig. 6L) than for SPEI03

330   (Fig. 6K). For the snow region, we see a notable effect of high temperatures: SEPI24 decreases with forest cover. Trees in mostly snow-covered regions change the albedo and the transpiration. Again, for the snow region, the model captures only a little part of the variability, which limits its interpretability.

    The combined forest fraction and meteorological effect on drought indices varies across regions and time scales τ in magnitude and direction. In equatorial and temperate regions, the long-term drought index (SPEI24) is primarily influenced by

335   precipitation, rather than forest cover. Similarly, the short-term drought index (SPEI03) in 4 regions is also more dependent on precipitation than on forest cover. However, in the arid region, temperature plays a significant role in modulating the short-term drought index (SPEI03), as well as the long-term drought index (SPEI24). Additionally, in temperate and snow regions, temperature also has a notable modulating effect on the long-term drought index (SPEI24).

4.3   Response of drought to precipitation and temperature under extreme forest fraction(minimum and maximum)

340   conditions

We studied the effect of precipitation and temperature on short-term (SPEI03) and long-term (SPEI24) drought indices for observed minimum ($\min(X_{\text{forest,region}})$) and maximum forest cover fractions ($\max(X_{\text{forest,region}})$). We generate a grid with $100\times$

100 points based on the variables of precipitation and temperature used in the linear models across different climate regions,
and then, use the precipitation, temperature, and forest extremes (maximum and minimum) to calculate the drought indices

345 (SPEI03 and SPEI24) based on the models from Eq. 5. The first two rows in Fig. 7 depict the short-term drought index (SPEI03)
obtained for the minimum (first row) and maximum forest cover (second row); the last two rows depict the long-term drought
index (SPEI24) for minimum (third row) and maximum forest cover (fourth row).
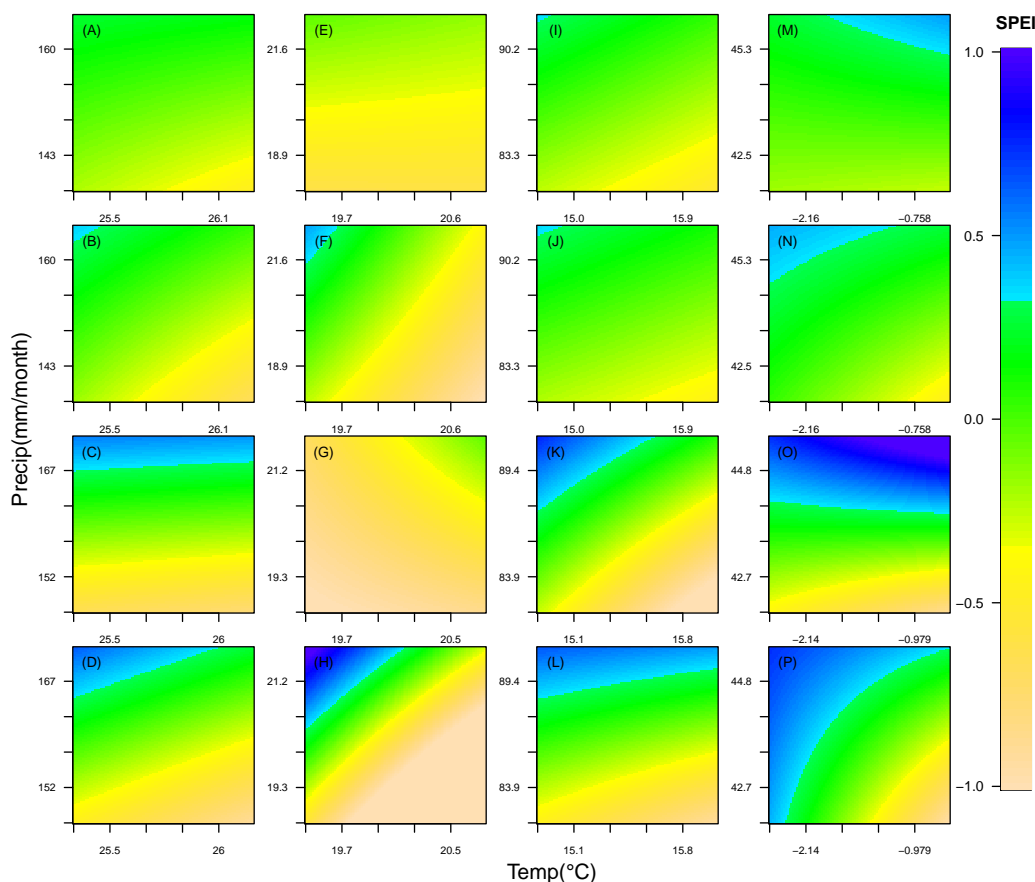
Figure 7. The variation of droughts (SPEI03: the first and second rows; SPEI24: the third and fourth rows) under the effect of minimal
(the first and third rows) and maximal (the second and fourth rows) forest cover across four regions (from the left to right: equatorial, arid,
temperate and snow regions)

Blue colors indicate the situations wetter than the median (positive indices), green represents situations close to the median
(indices around 0), and yellow indicates conditions drier than the median conditions (negative indices). For the equatorial

350 region, precipitation influences the short and long-term drought indices (vertical color change); for maximum forest cover
(Fig. 7B), the dependence on temperature (horizontal color change) becomes visible, even more so for the long-term index
(Fig. 7D). The long-term index in the arid region shows a somewhat stronger temperature dependence for maximum forest

cover (Fig. 7H) than that in the equatorial region (Fig. 7D). For minimum forest cover (Fig. 7G), the temperature dependence is very weak (and reversed). For SPEI03 (Fig. 7E and F), the dependence also changes from precipitation to temperature if

355 there are more trees. In the temperate region, the SPEI24 for minimum forest cover (Fig. 7K) shows the strongest temperature and precipitation dependence; increasing forest cover to maximum (Fig. 7L) significantly reduces the temperature dependence, leaving the long-term drought index for the temperate region dominated by precipitation. The short-term index (Fig. 7I and J) is less dependent on both, and the influence from precipitation and temperature is almost unaffected by the change in forest cover. In the snow region, the relationship between temperature, precipitation, and long-term droughts is closely linked to the extent

360 of forest cover. Maintaining maximum forest cover is crucial in strengthening the effects of temperature and precipitation on droughts (Fig. 7P). Minimizing the forest cover (Fig. 7O) eliminates the temperature dependence. For SPEI03 (Fig. 7M and N), the dependence on both variables is a lot weaker, with temperature dependence being reversed by reducing the forest from maximum (Fig. 7N) to the minimum (Fig. 7M).

Comparing all panels in Fig. 7, forest cover has a greater influence on the long-term drought index in the snow region.

365 Increasing the forest cover increases the dependence on temperature in snow, arid and equatorial regions, and it reduces the dependence on temperature for the temperate region.

Fig. 5 presents that the droughts indices are greatly affected by precipitation (except arid regions). In most cases, the color change in Fig. 7 should be more vertical. Transpiration from the forest is essentially the evaporation of water vapors from plant leaves and stems, which is an important part of the water cycle (39% of terrestrial precipitation and 61% of evapotranspira-

370 tion globally) (Schlesinger and Jasechko, 2014). within the cycle, temperature plays a major role in the rate of transpiration (Kimball, 1999), especially during the growing season. Using forests as a medium, the temperature effect would be more pronounced in the water cycle in most cases, as shown in snow, arid and equatorial regions. In the temperate region, the drought indices are dominated by precipitation and the forest only affects the influence of temperature to SPEI24, and when there are fewer trees, the influence of temperature will be amplified (shown in Fig. 6L). And this is consistent in Fig. 7K and L. Note:

375 simultaneously with afforestation or deforestation the global climate is changing. Therefore, local changes in climate may also be additionally influenced by global climate change and not only afforestation or deforestation rates.

5 Conclusions

The scientific community has dedicated significant efforts to quantify the influence of land cover changes on climate. In this study, linear models were employed to evaluate the impacts of forest cover and climatic factors on droughts at various temporal

380 scales in four distinct climate regions (excluding the polar region, which has negligible forest cover). The study findings are summarized as follows:

1. Linear models incorporating forest fraction, precipitation, and temperature yield the most accurate results for explaining drought indicators in the equatorial region, but are less effective in the snow region. These three variables provide a better fit for changes in SPEIs compared to scPDSI, which may be due to scPDSI's consideration of soil conditions.

385   Precipitation is the primary factor explaining a significant proportion of the regression variance in all regions, except for the arid region where temperature is the dominant factor.

2. It is conceivable that changes in precipitation and temperature can impact the relationship between forest cover changes and drought occurrence. Specifically, precipitation alters the influence of forest cover on long-term drought (SPEI24) in arid and snow regions, while temperature significantly modifies the effect of forest cover on both short- and long-

390   term droughts (SPEI03 and SPEI24) in the arid region and on long-term drought (SPEI24) only in temperate and snow regions.

3. Forest cover has differing effects on drought occurrence (especially long-term drought) depending on the maximum and minimum levels of forest fraction in different climate regions. Specifically, in equatorial, arid, and snow regions, higher forest cover intensifies the combined influence of precipitation and temperature for long-term drought. Conversely, in

395   regions with lower forest cover, precipitation is the dominant factor for drought occurrence. The opposite pattern is observed in the temperate region, where lower forest cover promotes a combined effect of precipitation and temperature for long-term drought.

Despite the substantial progress made in understanding the factors that influence drought occurrence, uncertainties remain that have not always been fully acknowledged. One source of uncertainty is the use of different drought indices, which can

400 produce divergent results. In this study, we focused on two indices, scPDSI and SPEI. However, the calculation of drought indices, particularly scPDSI, is subject to various uncertainties. For example, scPDSI requires information on temperature, precipitation, and soil conditions. Obtaining detailed soil information for each location can be challenging, leading to potential inaccuracies in the calculation of the index. In addition, human activities like irrigation are not accounted for in the index calculation, which can affect its accuracy. Meanwhile, each of the drought indices has its own niche where it excels. Different

405 drought indices should be used when assessing different types of droughts (Mishra and Singh, 2010). Secondly, this study used a relatively short-term dataset of 25-26 years, and future studies can use longer-term data to obtain a more robust understanding of the relationship between forest cover and drought. Finally, this study utilized linear models with a limited number of predictors, and future studies can investigate more complex models to explore other potential effects of forest cover change on drought. These gaps in knowledge present opportunities for future research and can help in developing a broader framework

410 for understanding natural hazards, including droughts.

Possible extensions of this study include broadening the scope of land cover analysis to include other types of land cover, such as agricultural land, grasslands, wetlands, and settlements. Additionally, conducting more specific research in particular locations, such as Europe, could provide more definitive recommendations. Future model inter-comparison studies, such as the Land-Use Model Intercomparison Project simulations (LUMIP; Lawrence et al., 2016) under the CMIP phase 6 (CMIP6), could

415 further investigate the impact of land use on climate and examine the effect of land cover change on the onset and evolution of drought under various forcing conditions. These extensions could significantly expand our understanding of the relationship between land cover change and drought and inform the development of more effective land use policies to mitigate the impacts of climate change. Expanding our understanding of the regional and global climate impact of land cover changes, including

their scale effects, can help to inform the development of land use policies that prioritize climate objectives. This is particularly
420 important given that decisions regarding land use are frequently made at the subnational level by regional authorities.

This study enhances our comprehension of the connection between forest cover and drought across various temporal scales and climatic regions. Additionally, it elucidates the combined impact of forest cover, temperature, and precipitation on drought variability. The findings of this study can offer a theoretical framework for the creation of regional land use policies that prioritize climate concerns, as well as deepen our insight into the impact of land surface changes on climate change.

425 *Code and data availability.* All the datasets in the article can be downloaded from the website for free. The links have been given in Sec. 2. The statistical analysis is finished by R. All the packages used in the paper are free and the information is given in Sec. 3.

Author contributions. YL and HWR conceived and designed the research. YL built the models with the primary processing data from BH, and conducted the statistical analysis under the supervision of HWR. YL made the figures. All authors interpreted the results and wrote the paper.

430 *Competing interests.* The authors declare that they have no conflict of interest.

Acknowledgements. YL acknowledges the support from the China Scholarship Council (CSC). BH acknowledges the support of the Norwegian Research Council (project no. 294534 and 286773).

References

Alkama, R. and Cescatti, A.: Biophysical climate impacts of recent changes in global forest cover, Science, 351, 600–604, 2016.

435 Allen, R. G., Pereira, L. S., Raes, D., Smith, M., et al.: Crop evapotranspiration-Guidelines for computing crop water requirements-FAO Irrigation and drainage paper 56, Fao, Rome, 300, D05 109, 1998.

Anderson, R. G., Canadell, J. G., Randerson, J. T., Jackson, R. B., Hungate, B. A., Baldocchi, D. D., Ban-Weiss, G. A., Bonan, G. B., Caldeira, K., Cao, L., Diffenbaugh, N. S., Gurney, K. R., Kueppers, L. M., Law, B. E., Luyssaert, S., and O'Halloran, T. L.: Biophysical considerations in forestry for climate protection, Frontiers in Ecology and the Environment, 9, 174–182, https://doi.org/10.1890/090179,

440 2011.

Anscombe, F. J.: The validity of comparative experiments, Journal of the royal statistical society. series A (General), 111, 181–211, 1948.

Bagley, J. E., Desai, A. R., Harding, K. J., Snyder, P. K., and Foley, J. A.: Drought and Deforestation: Has Land Cover Change Influenced Recent Precipitation Extremes in the Amazon?, Journal of Climate, 27, 345–361, https://doi.org/10.1175/Jcli-D-12-00369.1, 2014.

Bala, G., Caldeira, K., Wickett, M., Phillips, T. J., Lobell, D. B., Delire, C., and Mirin, A.: Combined climate and carbon-cycle effects of

445 large-scale deforestation, Proceedings of the National Academy of Sciences, 104, 6550–6555, https://doi.org/10.1073/pnas.0608998104, 2007.

Barichivich, J., Osborn, T., Harris, I., Van Der Schrier, G., and Jones, P.: Monitoring global drought using the self-calibrating Palmer Drought Severity Index [in" State of the Climate in 2020"], Bulletin of the American Meteorological Society, 102, S68–S70, 2021.

Beringer, J., Chapin, F. S., Thompson, C. C., and McGuire, A. D.: Surface energy exchanges along the tundra-forest transition and feedbacks

450 to climate, Agricultural and Forest Meteorology, 131, 143–161, https://doi.org/https://doi.org/10.1016/j.agrformet.2005.05.006, 2005.

Bonan, G. B.: Forests and climate change: forcings, feedbacks, and the climate benefits of forests, Science, 320, 1444–9, https://doi.org/10.1126/science.1155121, 2008.

Bryan, B. A., Gao, L., Ye, Y. Q., Sun, X. F., Connor, J. D., Crossman, N. D., Stafford-Smith, M., Wu, J. G., He, C. Y., Yu, D. Y., Liu, Z. F., Li, A., Huang, Q. X., Ren, H., Deng, X. Z., Zheng, H., Niu, J. M., Han, G. D., and Hou, X. Y.: China's response to a national land-system

455 sustainability emergency, Nature, 559, 193–204, https://doi.org/10.1038/s41586-018-0280-2, gm6bl Times Cited:184 Cited References Count:137, 2018.

Burke, E. J., Brown, S. J., and Christidis, N.: Modeling the recent evolution of global drought and projections for the twenty-first century with the Hadley Centre climate model, Journal of Hydrometeorology, 7, 1113–1125, 2006.

Chambers, J. and Hastie, T.: Linear models. Chapter 4 of statistical models in S, Wadsworth & Brooks/Cole, 1992, 1992.

460 Cherubini, F., Huang, B., Hu, X., Tölle, M. H., and Strømman, A. H.: Quantifying the climate response to extreme land cover changes in Europe with a regional model, Environmental Research Letters, 13, 074 002, 2018.

Cook, B. I., Smerdon, J. E., Seager, R., and Coats, S.: Global warming and 21 st century drying, Climate Dynamics, 43, 2607–2627, 2014.

Crowther, T. W., Glick, H. B., Covey, K. R., Bettigole, C., Maynard, D. S., Thomas, S. M., Smith, J. R., Hintler, G., Duguid, M. C., Amatulli, G., Tuanmu, M. N., Jetz, W., Salas, C., Stam, C., Piotto, D., Tavani, R., Green, S., Bruce, G., Williams, S. J., Wiser, S. K., Huber, M. O.,

465 Hengeveld, G. M., Nabuurs, G. J., Tikhonova, E., Borchardt, P., Li, C. F., Powrie, L. W., Fischer, M., Hemp, A., Homeier, J., Cho, P., Vibrans, A. C., Umunay, P. M., Piao, S. L., Rowe, C. W., Ashton, M. S., Crane, P. R., and Bradford, M. A.: Mapping tree density at a global scale, Nature, 525, 201–205, https://doi.org/10.1038/nature14967, 2015.

Dai, A.: Drought under global warming: a review, Wiley Interdisciplinary Reviews: Climate Change, 2, 45–65, 2011.

Dai, A.: Increasing drought under global warming in observations and models, Nature Climate Change, 3, 52, 2013.

470 Field, C. B., Lobell, D. B., Peters, H. A., and Chiariello, N. R.: Feedbacks of Terrestrial Ecosystems to Climate Change, Annual Review of
       Environment and Resources, 32, 1–29, https://doi.org/10.1146/annual.energy.32.053006.141119, 2007.

Findell, K. L., Berg, A., Gentine, P., Krasting, J. P., Lintner, B. R., Malyshev, S., Santanello, J. A., and Shevliakova, E.: The impact of
       anthropogenic land use and land cover change on regional climate extremes, Nature communications, 8, 989, 2017.

Ge, J., Guo, W. D., Pitman, A. J., De Kauwe, M. G., Chen, X. L., and Fu, C. B.: The Nonradiative Effect Dominates Local Surface Tem-
475   perature Change Caused by Afforestation in China, Journal of Climate, 32, 4445–4471, https://doi.org/10.1175/Jcli-D-18-0772.1, ie8vu
       Times Cited:21 Cited References Count:69, 2019.

Hansen, M. C., Stehman, S. V., and Potapov, P. V.: Quantification of global gross forest cover loss, Proceedings of the National Academy of
       Sciences, 107, 8650–8655, 2010.

Hansen, M. C., Potapov, P. V., Moore, R., Hancher, M., Turubanova, S., Tyukavina, A., Thau, D., Stehman, S., Goetz, S., Loveland, T. R.,
480   et al.: High-resolution global maps of 21st-century forest cover change, science, 342, 850–853, 2013.

Harris, I., Jones, P. D., Osborn, T. J., and Lister, D. H.: Updated high-resolution grids of monthly climatic observations–the CRU TS3. 10
       Dataset, International journal of climatology, 34, 623–642, 2014.

Hoek van Dijke, A. J., Herold, M., Mallick, K., Benedict, I., Machwitz, M., Schlerf, M., Pranindita, A., Theeuwen, J. J. E., Bastin,
       J.-F., and Teuling, A. J.: Shifts in regional water availability due to global tree restoration, Nature Geoscience, 15, 363–368,
485   https://doi.org/10.1038/s41561-022-00935-0, 2022.

Hu, X., Huang, B., Verones, F., Cavalett, O., and Cherubini, F.: Overview of recent land-cover changes in biodiversity hotspots, Frontiers in
       Ecology and the Environment, 19, 91–97, https://doi.org/10.1002/fee.2276, qo8br Times Cited:1 Cited References Count:32, 2020.

Huang, B., Hu, X., Fuglstad, G.-A., Zhou, X., Zhao, W., and Cherubini, F.: Predominant regional biophysical cooling from recent land cover
       changes in Europe, Nature communications, 11, 1–13, 2020.

490 Jones, D. A., Wang, W., and Fawcett, R.: High-quality spatial climate data-sets for Australia, Australian Meteorological and Oceanographic
       Journal, 58, 233, 2009.

Keyantash, J. and Dracup, J. A.: The quantification of drought: an evaluation of drought indices, Bulletin of the American Meteorological
       Society, 83, 1167–1180, 2002.

Kim, D.-H., Sexton, J. O., and Townshend, J. R.: Accelerated deforestation in the humid tropics from the 1990s to the 2000s, Geophysical
495   Research Letters, 42, 3495–3501, 2015.

Kimball, J. W.: Kimball's biology pages, Kimball, John W., 1999.

Li, Y., Zhao, M., Motesharrei, S., Mu, Q., Kalnay, E., and Li, S.: Local cooling and warming effects of forests based on satellite observations,
       Nat Commun, 6, 6603, https://doi.org/10.1038/ncomms7603, 2015.

Li, Y., Zhao, M., Mildrexler, D. J., Motesharrei, S., Mu, Q., Kalnay, E., Zhao, F., Li, S., and Wang, K.: Potential and Actual impacts of
500   deforestation and afforestation on land surface temperature, Journal of Geophysical Research: Atmospheres, 121, 2016.

Mahmood, R., Pielke, R. A., Hubbard, K. G., Niyogi, D., Dirmeyer, P. A., McAlpine, C., Carleton, A. M., Hale, R., Gameda, S., Beltrán-
       Przekurat, A., et al.: Land cover changes and their biogeophysical effects on climate, International journal of climatology, 34, 929–953,
       2014.

Maidment, D. R. et al.: Handbook of hydrology, vol. 9780070, McGraw-Hill New York, 1993.

505 McCullagh, P. and Nelder, J.: Generalized Linear Models, CRC Press, Boca Raton, Fla, 2 edn., 1989.

McKee, T. B., Doesken, N. J., Kleist, J., et al.: The relationship of drought frequency and duration to time scales, in: Proceedings of the 8th
       Conference on Applied Climatology, vol. 17, pp. 179–183, American Meteorological Society Boston, MA, 1993.

Mishra, A. K. and Singh, V. P.: A review of drought concepts, Journal of hydrology, 391, 202–216, 2010.

Naumann, G., Alfieri, L., Wyser, K., Mentaschi, L., Betts, R., Carrao, H., Spinoni, J., Vogt, J., and Feyen, L.: Global changes in drought
510   conditions under different levels of warming, Geophysical Research Letters, 45, 3285–3296, 2018.

Nepstad, D., Soares-Filho, B. S., Merry, F., Lima, A., Moutinho, P., Carter, J., Bowman, M., Cattaneo, A., Rodrigues, H., Schwartzman, S.,
McGrath, D. G., Stickler, C. M., Lubowski, R., Piris-Cabezas, P., Rivero, S., Alencar, A., Almeida, O., and Stella, O.: Environment. The
end of deforestation in the Brazilian Amazon, Science, 326, 1350–1, https://doi.org/10.1126/science.1182108, 2009.

Nepstad, D. C., Tohver, I. M., Ray, D., Moutinho, P., and Cardinot, G.: Mortality of large trees and lianas following experimental drought in
515   an Amazon forest, Ecology, 88, 2259–2269, 2007.

Peel, M. C., Finlayson, B. L., and McMahon, T. A.: Updated world map of the Köppen-Geiger climate classification, Hydrology and earth
system sciences, 11, 1633–1644, 2007.

Peng, S. S., Piao, S., Zeng, Z., Ciais, P., Zhou, L., Li, L. Z., Myneni, R. B., Yin, Y., and Zeng, H.: Afforestation in China cools local land
surface temperature, Proc Natl Acad Sci U S A, 111, 2915–9, https://doi.org/10.1073/pnas.1315126111, 2014.

520 Perugini, L., Caporaso, L., Marconi, S., Cescatti, A., Quesada, B., de Noblet-Ducoudre, N., House, J. I., and Arneth, A.: Biophysical effects
on temperature and precipitation due to land cover change, Environmental Research Letters, 12, 053 002, 2017.

Peterson, T. C. and Vose, R. S.: An overview of the Global Historical Climatology Network temperature database, Bulletin of the American
Meteorological Society, 78, 2837–2850, 1997.

Peterson, T. C., Heim Jr, R. R., Hirsch, R., Kaiser, D. P., Brooks, H., Diffenbaugh, N. S., Dole, R. M., Giovannettone, J. P., Guirguis, K.,
525   Karl, T. R., et al.: Monitoring and understanding changes in heat waves, cold waves, floods, and droughts in the United States: state of
knowledge, Bulletin of the American Meteorological Society, 94, 821–834, 2013.

Pitman, A. J., Avila, F. B., Abramowitz, G., Wang, Y. P., Phipps, S. J., and de Noblet-Ducoudre, N.: Importance of background climate in
determining impact of land-cover change on regional climate, Nature Climate Change, 1, 472–475, https://doi.org/10.1038/Nclimate1294,
871lt Times Cited:135 Cited References Count:25, 2011.

530 Popp, A., Calvin, K., Fujimori, S., Havlik, P., Humpenöder, F., Stehfest, E., Bodirsky, B. L., Dietrich, J. P., Doelmann, J. C., Gusti, M., et al.:
Land-use futures in the shared socio-economic pathways, Global Environmental Change, 42, 331–345, 2017.

Poulter, B., MacBean, N., Hartley, A., Khlystova, I., Arino, O., Betts, R., Bontemps, S., Boettcher, M., Brockmann, C., Defourny, P., Hage-
mann, S., Herold, M., Kirches, G., Lamarche, C., Lederer, D., Ottle, C., Peters, M., and Peylin, P.: Plant functional type classification for
earth system models: results from the European Space Agency's Land Cover Climate Change Initiative, Geoscientific Model Development,
535   8, 2315–2328, https://doi.org/10.5194/gmd-8-2315-2015, co1lq Times Cited:22 Cited References Count:69, 2015.

R Core Team: R: A Language and Environment for Statistical Computing, R Foundation for Statistical Computing, Vienna, Austria, https:
//www.R-project.org/, 2018.

Salati, E. and Nobre, C. A.: Possible climatic impacts of tropical deforestation, Climatic Change, 19, 177–196,
https://doi.org/10.1007/BF00142225, 1991.

540 Santoro, M., Kirches, G., Wevers, J., Boettcher, M., Brockmann, C., Lamarche, C., and Defourny, P.: Land Cover CCI: Product User Guide
Version 2.0, 2017.

Schlesinger, W. H. and Jasechko, S.: Transpiration in the global water cycle, Agricultural and Forest Meteorology, 189, 115–117, 2014.

Seneviratne, S. I.: Climate science: Historical drought trends revisited, Nature, 491, 338, 2012.

Shaxson, F. and Barber, R.: Optimizing soil moisture for plant production: The significance of soil porosity, Rome, Italy: UN-FAO, 2003.

545 Silva Dias, M. A., Avissar, R., and Silva Dias, P.: Modeling the regional and remote climatic impact of deforestation, Washington DC American Geophysical Union Geophysical Monograph Series, 186, 251–260, https://doi.org/10.1029/2008GM000817, 2009.

Snyder, P. K., Delire, C., and Foley, J. A.: Evaluating the influence of different vegetation biomes on the global climate, Climate Dynamics, 23, 279–302, https://doi.org/10.1007/s00382-004-0430-0, 859nf Times Cited:205 Cited References Count:60, 2004.

Staal, A., Flores, B. M., Aguiar, A. P. D., Bosmans, J. H., Fetzer, I., and Tuinenburg, O. A.: Feedback between drought and deforestation in
550 the Amazon, Environmental Research Letters, 15, 044 024, 2020.

Thornthwaite, C. W.: An approach toward a rational classification of climate, Geographical review, 38, 55–94, 1948.

Tian, L., Zhang, B. Q., Wang, X. J., Chen, S. Y., and Pan, B. T.: Large-Scale Afforestation Over the Loess Plateau in China Contributes to the Local Warming Trend, Journal of Geophysical Research-Atmospheres, 127, https://doi.org/ARTN e2021JD035730 10.1029/2021JD035730, ye2ld Times Cited:1 Cited References Count:71, 2022.

555 Trenberth, K. E., Dai, A., Van Der Schrier, G., Jones, P. D., Barichivich, J., Briffa, K. R., and Sheffield, J.: Global warming and changes in drought, Nature Climate Change, 4, 17, 2014.

van der Schrier, G., Barichivich, J., Briffa, K., and Jones, P.: A scPDSI-based global data set of dry and wet spells for 1901–2009, Journal of Geophysical Research: Atmospheres, 118, 4025–4048, 2013.

Vicente-Serrano, S. M., Beguería, S., and López-Moreno, J. I.: A multiscalar drought index sensitive to global warming: the standardized
560 precipitation evapotranspiration index, Journal of climate, 23, 1696–1718, 2010a.

Vicente-Serrano, S. M., Beguería, S., López-Moreno, J. I., Angulo, M., and El Kenawy, A.: A new global 0.5 gridded dataset (1901–2006) of a multiscalar drought index: comparison with current drought index datasets based on the Palmer Drought Severity Index, Journal of Hydrometeorology, 11, 1033–1043, 2010b.

Vicente-Serrano, S. M., Lopez-Moreno, J.-I., Beguería, S., Lorenzo-Lacruz, J., Sanchez-Lorenzo, A., García-Ruiz, J. M., Azorin-Molina, C.,
565 Morán-Tejeda, E., Revuelto, J., Trigo, R., et al.: Evidence of increasing drought severity caused by temperature rise in southern Europe, Environmental Research Letters, 9, 044 001, 2014.

Wallace, J., Jackson, N., and Ong, C.: Modelling soil evaporation in an agroforestry system in Kenya, Agricultural and Forest meteorology, 94, 189–202, 1999.

Wayne, C. P.: Meteorological drought, US weather bureau research paper, 58, 1965.

570 Wells, N., Goddard, S., and Hayes, M. J.: A self-calibrating Palmer drought severity index, Journal of Climate, 17, 2335–2351, 2004.

Wilkinson, G. and Rogers, C.: Symbolic description of factorial models for analysis of variance, Journal of the Royal Statistical Society: Series C (Applied Statistics), 22, 392–399, 1973.

Wilks, D. S.: Statistical methods in the atmospheric sciences, Elsevier, Amsterdam, NL, 4th edn., 2019.

Zhao, T. and Dai, A.: The magnitude and causes of global drought changes in the twenty-first century under a low–moderate emissions
575 scenario, Journal of climate, 28, 4490–4512, 2015.